Published in final edited form as:
Nat Nanotechnol. 2019 April ; 14(4): 362–368. doi:10.1038/s41565-018-0360-3.

Synthesis of metal-doped nanoplastics and their utility to investigate fate and behavior in complex environmental systems

Denise M. Mitrano[*,1], **Anna Beltzung**[2], **Stefan Frehland**[1], **Michael Schmiedgruber**[1], **Alberto Cingolani**[2], and **Felix Schmidt**[1]

[1]Process Engineering, Eawag – Swiss Federal Institute of Aquatic Science and Technology, Process Engineering, Uberlandstrasse 133, 8600 Dubendorf, Switzerland [2]Department of Chemistry and Applied Biosciences, Institute for Chemical and Bioengineering, ETH Zurich, Zurich, Switzerland

Abstract

Research on the distribution and effects of particulate plastic has intensified in recent years yet, due to analytical challenges, understanding of nanoplastic occurrence and behavior has remained comparatively elusive. However, process studies could greatly aid in defining key parameters for nanoplastic interactions within and transfers between technical and environmental compartments. Here, we provide a method to synthesize nanoplastic particles doped with a chemically entrapped metal used as a tracer, which provides a robust way to more easily, accurately and quantitatively detect nanoplastic in complex media. We show the utility of this approach in batch studies simulating the activated sludge process of a municipal wastewater treatment plant to better understand the fate of nanoplastics in urban environments. We found that the majority of particles were associated with the sludge (>98%), with an average recovery of over 93% of the spiked material achieved. We believe that this approach can be developed further to study the fate, transport, mechanistic behavior and biological uptake of nanoplastics in a variety of systems on different scales.

As the prominence of plastic as an environmental pollutant grows, efforts on several facets of particulate plastic (nano- and microplastic particles and fibers) research has begun to intensify to better understand their sources, fate and transport, as well as biological uptake and effects. Given that both primary plastic particles and secondary plastic debris come in a

[*]Corresponding author information: denise.mitrano@eawag.ch.

Data Availability

The data that support the plots within this paper and other findings of this study are available from the corresponding author upon reasonable request

Author Contributions

DMM conceived of the study, was involved in particle synthesis and characterization, WWTP batch experiments, wrote the manuscript and lead the research team. AB synthesized nanoplastics and contributed to manuscript writing. SF performed WWTP batch studies and contributed to manuscript writing. MS assisted in study design. AC was involved in particle synthesis and contributed to writing the manuscript. FS performed early fundamental tests for the experimental work. All authors have given approval to the final version of the manuscript.

Europe PMC Funders Author Manuscripts

broad spectrum of sizes, nanoplastics,[1,2] are also suspected to be present in the environment.[3,4] Recently, there have been developments specifically aimed to investigate this smaller size fraction of particulate plastic,[4–7] although analytical methods to measure nanoplastic in the environment remain comparatively elusive compared to the possibilities which exist for e.g. microplastics.[8–10] Some novel methods to detect nanoplastics have begun to come online,[11,12] but because (nano)plastics may be in dilute concentrations, improved sampling techniques (including sample concentration) need to be tackled in conjunction with lowering particle size detection limits.[11]

Few studies on nanoplastics natively in the environment have been performed while these developments are underway,[13] but knowledge on the sources, fate and transport can help identify which domains could be most affected.[14] Laboratory studies can aid in defining key parameters for transfers between particular technical or environmental compartments. For example, evaluating the flux of nanoplastics in municipal waste water treatment plants (WWTP), which are considered hubs between the urban and natural environments, would better determine if nanoplastics are released to receiving waters or are retained in the sludge. Primary nanoplastics have a number of demonstrated applications, including shell structures for encapsulating dyes,[15] additives in cosmetics[15–17] and shampoos[18], and to transport fragrances in e.g. laundry detergents and fabric softeners.[19,20] Many of these primary nanoplastics will be released directly to sewers during consumer use. While bans restricting the use of particulate plastic in ‘rinse-off’ products have recently been passed in some countries,[21] specific regulation and enforcement is neither complete nor global, with many potential loopholes and limitations in scope.[22] Secondary nanoplastics are also present in the environment,[1,5] ranging from tire wear[23,24] to fragmented mismanaged waste[25]. These sources of plastic will make their way to the WWTP through road run-off in locations which have combined sewer systems.[26]

While progress is still ongoing to measure nanoplastics in field studies, researchers who study the fate, transport and biological interactions/effects of nanoplastics in bench top or pilot scale studies can take advantage of an entirely different approach. Doping particles with a tracer can be an effective way to track particles that are difficult to analyze due to low concentrations, impeded by high natural backgrounds, or in the case of nanoplastic, limited analytical techniques which exist to identify them in complex matrices.[27] In this study, we synthesized nanoplastics particles with a chemically entrapped metallic fingerprint which can greatly aid studies to understand underlying mechanisms, processes and principals of nanoplastic behavior. Using a scarce metal has several key advantages including; homogenization or digestion of complex samples will not quench the tracer (as is often the case with fluorescence[28]) and standard methods for trace metal analytics already exist and can be exploited for measuring metal-laden plastic materials. Moreover, when using a scarce metal, the particles can be spiked directly into a variety of environmental samples without worry of high (metal or plastic) background interferences.[29]

In this study, a suite of detailed particle characterization and testing was performed to show the stability of the nanoplastics over time. The characterization regime included particle imaging (SEM, STEM-EDX), sizing (DLS, electron microscopy), and metal (Pd) incorporation (ICP-MS). These measurements allowed us to: 1) ensure metal loading per

Europe PMC Funders Author Manuscripts

particle (and thus the entire solution) was even, 2) calculate the detection limit both in terms of total Pd and nanoplastic particle concentrations, and 3) ensure Pd was not leaching from the particles over time. In terms of application, batch studies were performed to simulate the activated sludge process of a municipal WWTP using real municipal wastewater from a continuously running pilot scale system on site. Here, three independent objectives were; 1) evaluating the evenness of particle distribution in well-mixed activated sludge (and thereby optimizing sampling protocol for nanoplastics), 2) determining the affinity for heteroaggregation of nanoplastics with the suspended solids in the sludge (i.e. surface affinity and how quickly nanoplastics adhere to sludge flocs) and 3) assessing total nanoplastic retention in WWTP (i.e. the fraction which was associated to the sludge versus the supernatant in batch reactors).

Nanoplastic synthesis and characterization

The general structure of the particles synthesized was a polyacrylonitrile (PAN) core material which contained the metal tracer, followed by the addition of a crosslinked polystyrene (PS) shell (Table S-1, Figure S-1). The reasoning for this multi-step process was to impart a few key benefits over a single batch emulsion including, 1) acrylonitrile (AN) is capable of chemically complexing the Pd in the water phase, 2) the core/shell structure would ensure there was minimal leaching of metal from the particle, and 3) the shell could be changed independently of the core (i.e. different styrene morphologies and/or different polymers could be added for the shell). The surface of the nanoplastic can be controlled by the composition and speed at which the shell polymer material(s) are fed into the reaction vessel (Figure S-2). When the shell is formed by feeding a mixture of acrylonitrile and styrene/DVB on a gradient to slowly transition between the two polymers, this results in a smooth surface (Figure 1B). Conversely, by directly adding styrene and DVB on the seed of the PAN core, phase separation of the polymer proceeds throughout the polymerization, because of their poor compatibility leading to a “raspberry” like appearance (Figure 1C).30 By feeding only styrene at the end of the synthesis, a complete styrenic outer layer was ensured for both morphologies. Additional information regarding reaction conversion rates, particle and metal concentrations in solution and nanoplastic size can be found in the supplemental information (Figure S-3). The combination of STEM/EDX allowed for a projection of the elemental distribution inside the particles. As expected, the metal Pd atoms are predominately in the center (i.e. core, Figure 1D) of the nanoplastics, with minimal Pd entrapment closer to the final particle surface (Figure 1, panels E and F). Additionally, the core/shell structure could be visualized since the polymer used for the core of the particle (PAN) contains nitrogen whereas the shell material (mainly) does not. This is clearer for the raspberry shell (Figure 1I) than for the smooth shell (Figure 1H) since the raspberry shell consists only of crosslinked polystyrene, and thus has a stark transition between the nitrile concentration in the polymers, whereas the smooth shell is a gradient from the nitrogen containing PAN to the nitrogen-free crosslinked polystyrene.

Nanoplastic metal incorporation and stability

When measuring serial dilutions of all particle variants by ICP-MS (Figure 2, panels A and B), a linear Pd response was achieved which indicates that; 1) particle concentration scales

linearly with Pd concentration, 2) Pd can be directly measured by ICP-MS and thus be a proxy for nanoplastic, 3) when combined with a calculation of the particle number in solution, the Pd loading per particle can be estimated, and 4) the detection limit can be calculated (both in terms of total Pd and, by extension, nanoplastic number concentration). To assess overall particle stability and potential leaching of Pd from the nanoplastics over time, dilute particle solutions in DI water were shaken end-over-end for two months. Subsamples were taken weekly to measure total particle concentration and to assess leached Pd, by means of measuring Pd content of the filtrate of centrifugal ultrafilters. Over eight weeks, we found that Pd concentrations did not change significantly, indicating that the particles are stable in DI H_20 at relevant exposure concentrations (Figure 2A and B). Additionally, both the particle size and zeta potential were stable over the all analysis time points (Table S-2). The detection limit in terms of Pd concentration in DI water was determined to be 0.005 μg/L, which related to approximately $9.8x10^8$ particles/L (Figure S-6). In the particle core-only solution, there was approximately 0.3% ionic Pd of the total Pd in solution that was not incorporated into the particle at the time of synthesis (Figure S-7). For raspberry and smooth shell nanoplastic suspensions, the relative amount of dissolved Pd to total Pd in the particles was below or close to the ICP-MS detection limit at time zero (for measured Pd concentrations in particle filtrates, see Figure S-7). Over time, there was a minimal increase of free Pd released into solution that was not associated with the particles, but over the course of two months the dissolved Pd did not exceed 0.5%.

Based on the absence of Pd leaching from the particle core, we can deduct that the Pd is sufficiently incorporated inside the polymer to be used as a conservative tracer. Previous work has indicated the presence of a chemical bond between Pd and AN, hence a chemical entrapment mechanism.31 Given the now proven stability of Pd into the core, other types of polymers could be grown on this base particle structure for other composite nanoplastic variants. There are several different monomers used in free radical polymerization, which are also of environmental interest, which could alternatively be added as a shell material in this system, namely, poly(styrene-butadiene) rubber (SBR) used in car tires and modified asphalt32–34, polyvinylchloride (PVC) used in electrical cables,35 construction or clothing, 36 and poly(styrene-acrylonitrile) (SAN) which is commonly used for kitchen utensils.37 By synthesizing these materials in nanoplastic form, this could mimic the breakdown products of larger plastic items. The chemistry or morphology of the outer shell would have no influence on the function/utility of the Pd as a tracer.

Nanoplastic assessment and behavior in WWTP mixed liquor

Batch reactors were fed with mixed liquor (activated sludge, approximately 2.5 g/L total suspended solids (TSS)) which was collected from the nitrification tank of a pilot scale WWTP on site on each experimental day, and used within one hour of collection to help preserve biological activity. For each of the experimental protocols below, 250 mL glass Schott bottles were filled with 200 mL freshly collected activated sludge, open to air and gently stirred with a spin bar. Depending on experimental aims, nanoplastics were spiked into the reactor at multiple concentrations and allowed to stir for various lengths of time, up to two hours, representing the residency time of activated sludge in our pilot plant.

Europe PMC Funders Author Manuscripts

Subsequently, stirring ceased and sludge was allowed to settle, representing the secondary clarifier of the WWTP.

Plastic evenness in mixed liquor – insight into sampling strategies

Digestion of nanoplastic in mixed liquor was reproducible at various concentrations using standard additions. Alongside this, one can determine if the nanoplastics are well distributed within the mixed liquor (i.e. no “hotspots” created), which could lead to large under- or overestimations of plastic recovery depending on the sampling size or location. Thus, a sampling protocol was designed to ensure correct 1) sample size, 2) number of sub-samples and 3) sampling location within the test vessel. As a comparison, the same concentration(s) of ionic Pd was also tested under these conditions, to evaluate digestion and sampling techniques. A complete recovery of metal and low standard deviation indicated that the material is evenly distributed through the mixed liquor and that sampling protocol gives precise results (Figure S-9).

Nanoplastic affinity for heteroaggretation

The removal of nanoplastics from suspension was measured by initial and final particle concentrations after mixing for an allocated amount of time (ranging between 1 min and 2 h), with subsequent settling for 30 min and sampling the supernatant. A basic estimate of the attachment of nanoplastics to organic matter can be made by evaluating the decrease of plastics in the supernatant with increased contact time between the nanoplastics and activated sludge. A linear regression can be fit to time points under 10 min (dashed line, Figure 3). Total removal of nanoplastics increased with mixing times of up to 30 min, after which point the removal stabilized for both particle morphologies. As suggested by the similar linear regression of the slopes in Figure 3, there was not a statistically significant difference in terms of removal for the different particle morphologies. Furthermore, there is little practical difference when considering the relative speed of particle attachment (minutes) to the residence time of the plastics in a real WWTP (hours). Both smooth and raspberry shelled nanoplastics had a similar total removal, with the vast majority of nanoplastics settling along with the sludge after 30 minutes of mixing time.

WWTP batch experiments- Depth Profile

The sludge layer formed after settling occurred in the batch reactors was visually not homogeneous, where there was a less dense sludge (TSS) at the top of supernatant/sludge interface and increasing density with depth (Figure 4A, Figure S10). The mass fraction of plastics recovered at each sampling depth correlated well with the TSS gradient for all concentrations of plastic spikes tested (Figure 4A), indicating that there is a direct correlation between mass of TSS and nanoplastic concentration. Furthermore, this analysis highlights the sensitivity of our method that we can clearly and precisely describe the nanoplastic concentration at discrete depths along a depth profile. Categorically, there was less than 1% of measured plastic in the supernatant (roughly representing WWTP effluent) and > 99% in the sludge layer. In total, 93 +/- 3% of the nanoplastic spiked was recovered across all concentrations and replicates (n=9). We wanted to assess if particles were still evenly attached to the sludge but it was the sludge settling pattern that was responsible for the observed plastic gradient with sludge depth. After the mixed liquor was allowed to settle,

the supernatant was decanted, the sludge was re-homogenized (so that the TSS gradient was removed) and the sludge was subsequently sampled over depth. The concentration of nanoplastics was then even with depth, again reinforcing the assessment that the nanoplastics are in direct association with the TSS (Figure 4B). This is an important consideration when determining an appropriate sampling strategy, as sub-sampling from the settled sludge without re-homogenization can give significantly different concentrations depending on slight changes of sampling location, and thus closing the mass balance becomes more challenging. While true replicates of a location cannot exist as the environment is by nature heterogeneous, our results indicate that even slight variations in sampling strategy (in this case, sampling depth) may lead to significantly different measured nanoplastic concentrations.

Utility of metal labeled nanoplastics for bench scale and pilot scale studies on nanoplastic

The explicit detection limits of other analytical techniques to measure particulate plastics are difficult to directly compare because authors can either present exposure concentrations or method detection limits in terms of plastic mass concentration or, alternatively, as particle number concentration detection limits.11,38 In terms of plastic mass, approximately 1 μg nanoplastic/L can be measured when using the materials produced here, based on the detection limit of Pd and relative concentration of Pd in the nanoplastic particle. Comparison between the number detection limits of particles of vastly different sizes can be somewhat misleading, given the intrinsic mass difference between nano- and microplastics. For example, using fluorescently labeled particles, detection limits between $7.5x10^4$ particles/L (for particles 20 μm in diameter)39 and $2.91x10^{11}$ particles/L (for particles 100 nm in diameter)28 have been reported. Effectively, the particles produced here have a particle number detection limit at least three orders of magnitude lower than other labeled particles of a similar size. Given that fluorescence was reported to change significantly during different digestion procedures,28 the metal incorporated particles proves to be a more reliable tracer, especially given the consistently high recovery in complex matrices (>90%). Additionally, since the Pd is securely entrapped inside the polymer, these particles are also suitable for ecotoxicity tests. Even at the highest testing concentration conducted here, the maximum concentration of Pd leached after eight weeks (0.05 μg/L; $4.7x10^{-4}$ μM) is five orders of magnitude below the reported EC_{50} values for free Pd and Pd complexes under a number of different conditions and target organisms.40

By using the metal fingerprint incorporated into the nanoplastics developed here, the possibility exists to repurpose some analytical techniques developed to measure inorganic nanoparticles in complex matrices, for example, single particle ICP-MS and Asymmetrical Flow Field Flow Fraction (AF4)-ICP-MS (see supplemental information for additional discussion and initial trials). Notably, the metal tracer itself cannot provide size, shape or polymer identity information alone. However, upon synthesis of a suite of particles with known sizes, shapes and polymers with various corresponding metals, divergent fate, transport, or biological interactions could be assessed at once in a given test system which was spiked with different metal-doped plastics.

Europe PMC Funders Author Manuscripts

Retention of nanoplastics in WWTP activated sludge

Physical-chemical processes controlling nanoplastic affinity (or attachment) to natural colloids will likely play key roles in determining if and how quickly nanoplastic particles adhere to larger materials in suspension and thus ultimately settle, affecting transport and fate over time and distance.41 Others have previously used the trends measured for particle affinity for heteroaggregation (surface affinity) to provide a value for attachment efficiency. 42,43 In this present case, the vast majority of nanoplastics heteroaggregate with sludge flocs within ten minutes. Given that the actual residency times of the mixed liquor and plastics in a WWTP are cumulatively much longer (hours) than the time shown for nanoplastic heteroaggregation (minutes), the attachment efficiency is of limited practical value because modeling attachment on a more time-resolved scale is not necessary for the process studied here. Furthermore, if an attachment efficiency of nanoplastics were to be derived for this system, it may not necessary be used to explicitly model nanoplastic fate in rivers, oceans, etc. because of different incidental particle characteristics.

Rather, the question we aim to answer through these experiments is to what extent nanoplastic is removed through the WWTP activated sludge process. Previous studies using inorganic engineered nanomaterials have also shown a good correlation between batch studies and pilot scale WWTP to accurately estimate particle retention in the sludge.42,44 By understanding the proportion of plastic that will exit the WWTP through different avenues (effluent or sludge), we can provide information for material flow modeling by way of transfer coefficients.45 If, as these batch studies suggest, over 99% of nanoplastics will be associated with sludge then appropriate concentrations of nanoplastics in WWTP effluent can be estimated, with further fate modeling for particle behavior in rivers, etc. Likewise, depending on locality, plastics in the sludge could be modeled to be applied to agricultural fields (with accumulation over subsequent years), or eliminated through sludge incineration.

While data is lacking on nanoplastic removal through real municipal WWTP, several studies have measured microplastics and found that a sizeable fraction (78-90%) were retained in the primary clarifier,46 with an additional decrease (7-20%) through the secondary treatment process.46,47 Nevertheless, even relatively low concentrations of plastics in the effluent can relate to higher concentrations of plastics downstream of the WWTP because of the high volume of effluent released daily.48,49 Often, technical constraints result in the omission of the smaller sized fraction of particulate plastic (i.e. sub-10 μm) being measured, yet this can result in reporting highly underestimated concentrations as it is estimated that between 35 – 90% of particulate plastic, on a number basis, are not currently being detected.50–53 When considering smaller sized particles in a WWTP, given the good retention of inorganic engineered nanoparticles in the sludge,44,54,55 coupled with the results of the batch studies from this present study, a high retention efficiency might also be anticipated for nanoplastics. Nevertheless, given that WWTP are continuously running, dynamic systems, using e.g. a pilot scale WWTP to more definitively assess the behavior of nanoplastics in a more comprehensive way is certainly warranted.

Conclusions

The theme of (particulate) plastic pollution has recently received considerable attention in the public media demonstrating the interest of our society in plastic waste. Vivid and emotional discussions on particulate plastic have also revealed a certain discomfort in the collective public audience due to the lack of clear statements about the extent of exposure and effects of particulate plastic on environmental (and human) health.56 Ultimately, one of the goals of many researches in this field today is to achieve an ecological risk assessments of plastic particles. Understanding exposure (including fate and transport) is one half of the risk equation. While the particles synthesized in this study cannot ultimately provide direct analytical tools to measure particulate plastic which is already in the environment, by providing the opportunity to quantitatively measure and track trace concentrations of nanoplastic in bench and pilot scale systems, they can make an excellent bridge for understanding environmental process or biological uptake of nanoplastics until analytical techniques for measuring environmental (nano)plastics have matured. For example, on the basis of these experiments, we can suggest that the nanoplastics which enter a WWTP will likely predominately leave the system through the sludge opposed to the effluent. Consequently, receiving waters would receive much fewer nanoplastic particles directly compared to concentrations which remained in the sludge, but variable sludge usage pathways by country (agricultural application, incineration) will deliver divergent sinks or elimination pathways of plastics from the WWTP.

Materials and methods

Materials

Acrylonitrile (AN, Aldrich chemistry ≥99.0%), styrene (ST, Sigma Aldrich ≥99.0%) and divinylbenzene (DVB, Sigma Aldrich ≥60.0%) were the monomers used for emulsion polymerization. Water-soluble potassium persulfate (KPS) (Merck, ACS, Reag. Ph. Eur) was employed as an initiator. Potassium poly(ethylene glycol) 4-nonylphenyl 3-sulfopropylether (KPE, Sigma Aldrich ≥99%) and sodium dodecyl sulfate (SDS, Sigma Aldrich ≥99%) were used as surfactants and stabilizers during different polymerization stages. A water-soluble Pd precursor was used, K_2PdCl_4 (ABCR, 99%). The reaction medium was deionized water for all syntheses and was stripped with N_2 *(g)* prior to the start of the polymerization. All materials were used without further purification. An ionic Pd standard solution (10000 mg/L, Sigma Aldrich) was diluted for a calibration solution for the ICP-MS from 0 to 10 μg/L, while an ionic In standard (Sigma Aldrich) was diluted to 100 μg/L as internal standard during sample analysis.

Polymer synthesis

The polymerization procedure consisted of a two-step emulsion polymerization, in which first the core particles were synthesized, after which a further shell was grown through feeding a second monomer solution over time (Figure S-1). Complete details are given in the supporting information, but briefly, the use of water-soluble materials including surfactants (SDS and KPE), initiator (KPS) and metal precursor (K_2PdCl_4) resulted in a chemical entrapment of the metal in the polymer. The evolution of the polymer conversion and

Europe PMC Funders Author Manuscripts

particle size were followed by thermogravimetric analysis (T= 120°C) using a Mettler Toledo (Switzerland) and by Dynamic Light Scattering (DLS) using a Malvern Zetasizer Nano Z (United Kingdom) with backscatter angle 173° at 25°C, respectively on an hourly basis (Figure S-2). For the nanoplastic core, surfactant (SDS) and initiator were charged inside the reactor and the dissolved metal precursor was fed into the reaction over the course of two minutes with a simple syringe when the nucleation point was initially achieved.31 At the outset of the synthesis, the KPE syringe was added at the same pace as the K_2PdCl_4. A conversion rate of monomer to polymer of 90% or over was established before shell addition began. The core particles acted as a seed for the further growth of the shell. Without stopping the core reaction, additional dissolved KPS was introduced directly by syringe after which a new feed of monomer mixture was connected to the reaction vessel, thus also diluting the mixture prior to further addition of monomers. Depending on the final morphology of the particle desired, different feed strategies were adopted. For a rough surface morphology (i.e. raspberry shell particles), a feed of water, styrene and DVB (see CFR in Table S-1) was directly connected without any further treatment and left dosing for four hours at a flow rate of 0.06 mL/min, with 20 g water (for 250 mL sized batch) added at two hours to reduce the risk of aggregation. To achieve a smooth surface morphology (i.e. smooth shell particles), a more gradual change of the feed composition was obtained with the usage of two pumps to provide a gradient between the initial core material (i.e. acrylonitrile) and transition to the styrene outer shell (Figure S-1). As was the case of the raspberry shell synthesis, after two hours of shell synthesis 20 g water was added to the reaction vessel. After the synthesis was complete, the latexes were directly filtered with a filter paper (MN 615, 22 s filtration speed) to remove all possible agglomerates. Finished nanoplastics were stored in plastic bottles at room temperature. We were successful in upscaling the synthesis to 1 L, with keeping the recipe similar.

Particle imaging and mapping elemental distributions

Scanning Electron Microscopy (SEM, Leo 1530, Zeiss, Germany) was employed at a voltage of 5 kV and using a SE in-lens detector. The samples were loaded onto a carbon sticker on a stub and then coated with Pt (4-5 nm) prior to analysis. Sizing of 1000 particles was done from the SEM images by the software ImageJ. To assess the metal dispersion and element distribution in the nanoplastics, scanning transmission electron microscopy and Energy-Dispersive X-ray spectroscopy (STEM-EDX) was performed on materials taken at two time points along the synthesis; after core formation and after the final shell formation (i.e. complete and final particle synthesis). Electron microscopy measurements were done on a FEI Talos F200X electron microscope equipped with a Super-X SDD detector at an acceleration voltage of 200 kV and using high angle annular dark field (HAADF). EDX hypermaps (spot size 6, voltage 200 kV, acquisition time 10 min, image resolution 1024x1024 pixels) were acquired using Esprit software (Bruker, Germany) up to 40 keV to assess the M and L lines of Palladium. In all cases, the signals of the individual atoms were enhanced by the software.

Particle characterization: size, surface properties and Pd incorporation

Particle Surface Charge (Zeta Potential) and stability (DLS)—Zeta potential and DLS measurements were performed on the Malvern Zetasizer with a disposable folded

capillary cell (DTS1070, Malvern) at all sample points of interest. The nanoplastic stock solution was diluted to approximately 0.5 mg/L particle concentration in ultrapure DI H_2O, with three sequential measurements lasting 120 seconds each. DLS data collection parameters are the same as those acquired during particle synthesis. Zeta potential and DLS measurements were also collected over time in association with the particle leaching experiments to assess particle stability in more dilute concentrations. The average zeta potential and standard deviation is reported here (Figure S3, Table S2).

Nanoplastic particle calibration curves, particle stability and particle leaching potential

In order to ensure the Pd tracer was fixed in the polymer and could be used as a conservative tracer over time, the stock nanoplastic solutions for both the particle core and the final core/shell structure(s) was diluted in ultrapure DI H_2O in glass vials with tightly fitting lids at three dilution factors (0.1 mg Pd/L, 0.5 mg Pd/L and 1 mg Pd/L, corresponding to particle concentrations of approximately $1.78x10^{13}$, $8.88x10^{13}$ and $1.78x10^{14}$ particles/L, respectively for the core and $1.24x10^{13}$, $6.22x10^{13}$ and $1.24x10^{14}$ for the shell particles). These solutions ranged from 500 to 5000 times dilution of the stock nanoplastic solution. The solutions were placed on an end-over-end shaker with samples taken at the outset of the experiment (i.e. time zero) and subsequently on a weekly basis for two months. The solution pH ranged from 6.6 for the least diluted to 6.9 for the most diluted particle suspension. At each sampling time, four analyses were performed. First, each solution was further diluted by a factor of 100 for ICP-MS analysis (final analysis nominal concentration of 1 μg/L, 5 μg/L and 10 μg/L Pd, particle concentrations of $1.78x10^{11}$, $8.88x10^{11}$ and $1.78x10^{12}$ particles/L, respectively for the core and $1.24x10^{11}$, $6.22x10^{11}$ and $1.24x10^{12}$ for the shell particles). The second analysis was using centrifugal ultrafilters (Sartorius Stedim, VIASPIN centrifugal filters, 10 kDa cutoff) of the final nanoplastic particle dilutions, with the filtrate measured by ICP-MS to determine the residual/leached Pd in each solution, presented here as a percentage of Pd in the nanoplastic particles of the corresponding solution. Finally, DLS and zeta potential measurements were recorded for each time point.

WWTP batch experiments and affinity for heteroaggregation

WWTP samples (effluent and mixed liquor) were collected from a continuously running pilot scale treatment plant at Eawag, which is fed with real municipal wastewater from the city of Dübendorf, Switzerland. Mixed liquor (activated sludge) samples were collected from the nitrification tank (approximately 2.5 g/L total suspended solids) on each experimental day, and used within one hour of collection to help preserve biological activity. Background Pd concentration in the mixed liquor was measured by ICP-MS as less than 25 ng/L daily. As a control for the batch experiments to ensure complete digestion of both matrix and (spiked) nanoplastic, as well as recovery of Pd, in complex media, aliquots of nanoplastic were directly digested in Teflon digestion tubes in the presence of 2 mL various matrices (DI H_2O, WWTP effluent, mixed liquor) and compared to the analysis of nanoplastics in ultra-pure DI H_20 (see supplemental information for further information on digestion procedure).

Three independent objectives were investigated in the batch experiments simulating the activated sludge process including, 1) evenness of particle distribution in well-mixed

activated sludge, 2) determining the affinity for heteroaggregation of nanoplastics with the suspended solids in the sludge (i.e. a simplified attachment assessment) and 3) estimation of the overall removal efficiency of nanoplastics during WWTP activated sludge treatment by measuring particles associated with the sludge versus those remaining in solution.

For the first objective of evaluating the evenness of nanoplastic distribution in the mixed liquor, 250 mL glass Schott bottles were filled with 200 mL freshly collected activated sludge, open to air and gently stirred with a spin bar. Three concentrations of nanoplastics ($1.24x10^{12}$, $6.22x10^{12}$ and $1.24x10^{13}$, corresponding to 10, 50 and 100 μg/L Pd) were spiked into different reactors (in triplicate). While a lower concentration of particles could have been spiked, we did not find it necessary to work close to the Pd detection limit to study particle fate. After two hours of continuous stirring, five, 1 mL aliquots were taken by pipette at random locations from the vial and subsequently digested and analyzed by ICP-MS for Pd content to assess 1) reproducibility of the sampling and 2) recovery of the nanoplastic.

To assess the rate of nanoplastic affinity to the suspended solids (the second objective), a series of batch reactors with 200 mL of mixed liquor with one concentration of nanoplastics ($6.2x10^{12}$ particles/L, in triplicate) were prepared for both raspberry and smooth nanoplastic shell morphologies. Mixing was stopped after 1 min, 3 min, 5 min, 7 min, 10 min, 15min, 30 min, 1 hr, 1.5 hr and 2 hr and the sludge was allowed to settle for 30 min, similar to experimental protocols in Barton et al.42 Triplicate aliquots of the supernatant (5 mL) were collected 2 cm below the air water interface, digested, and analyzed by ICP-MS to assess the proportion of nanoplastics remaining in solution over time. A linear regression was fit to time points to assess attachment.43,44

For the third objective, to estimate the overall retention of nanoplastics in the sludge, the mixed liquor set-up described in objective one was allowed to stir for two hours, the approximate residence time of activated sludge in one stage of the pilot scale WWTP at Eawag. Raspberry shell nanoplastics were used throughout all experiments. After two hours, vials were left to settle for 30 min before sampling commenced. Sequential 5 mL samples were taken from the air-water-interface for the entirety of the 200 mL of the solution (40 samples) in order to create a depth profile of plastic presence in the settled mixed liquor. After all the sludge was sampled, the Schott bottle was rinsed three times with 5 mL of DI H_20 to analyze remaining material. Both depth profile samples and bottle rinses were digested and analyzed by ICP-MS. In a variant of this experimental set up, to remove the total suspended solid (TSS) gradient in the settled sludge fraction to assess if nanoplastic was correlated with TSS concentration, after settling the supernatant was decanted, the sludge was re-homogenized and sampled sequentially without (re-)settling. In a separate container, TSS measurements were taken along the (settled) depth profile with drying 10 mL aliquots of solution on a 0.45 μm filter paper in sequence.

Supplementary Material

Refer to Web version on PubMed Central for supplementary material.

Europe PMC Funders Author Manuscripts

Acknowledgements

We would like to thank Ralf Kägi and Mark Surette for providing discussions and feedback, Massimo Morbidelli for access and equipment to synthesize the particles, Giuseppe Storti for discussions, Lu Jin for preliminary particle synthesis and Hua Wu for facilitating this collaboration.

References

1. Lambert S, Wagner M. Characterisation of nanoplastics during the degradation of polystyrene. Chemosphere. 2016; 145:265–268. [PubMed: 26688263]
2. Gigault J, et al. Current opinion: What is a nanoplastic? Environmental Pollution. 2018; 235:1030–1034. [PubMed: 29370948]
3. da Costa JP, Santos PS, Duarte AC, Rocha-Santos T. (Nano) plastics in the environment–sources, fates and effects. Science of The Total Environment. 2016; 566:15–26. [PubMed: 27213666]
4. Mattsson, K, Jocic, S, Doverbratt, I, Hansson, L-A. Microplastic Contamination in Aquatic Environments. Elsevier; 2018. 379–399.
5. Gigault J, Pedrono B, Maxit B, Ter Halle A. Marine plastic litter: the unanalyzed nano-fraction. Environmental Science: Nano. 2016; 3:346–350.
6. Oriekhova O, Stoll S. Heteroaggregation of nanoplastic particles in the presence of inorganic colloids and natural organic matter. Environmental Science: Nano. 2018; 5:792–799.
7. Alimi OS, Farner Budarz J, Hernandez LM, Tufenkji N. Microplastics and nanoplastics in aquatic environments: aggregation, deposition, and enhanced contaminant transport. Environmental science & technology. 2018; 52:1704–1724. [PubMed: 29265806]
8. Dümichen E, et al. Fast identification of microplastics in complex environmental samples by a thermal degradation method. Chemosphere. 2017; 174:572–584. [PubMed: 28193590]
9. Hidalgo-Ruz V, Gutow L, Thompson RC, Thiel M. Microplastics in the marine environment: a review of the methods used for identification and quantification. Environmental science & technology. 2012; 46:3060–3075. [PubMed: 22321064]
10. Shim WJ, Hong SH, Eo SE. Identification methods in microplastic analysis: a review. Analytical Methods. 2017; 9:1384–1391.
11. Mintenig SM, Bauerlein P, Koelmans AA, Dekker SC, van Wezel A. Closing the gap between small and smaller: Towards a framework to analyse nano-and microplastics in aqueous environmental samples. Environmental Science: Nano. 2018
12. Gigault J, El Hadri H, Reynaud S, Deniau E, Grassl B. Asymmetrical flow field flow fractionation methods to characterize submicron particles: application to carbon-based aggregates and nanoplastics. Analytical and bioanalytical chemistry. 2017; 409:6761–6769. [PubMed: 28948363]
13. Ter Halle A, et al. Nanoplastic in the North Atlantic subtropical gyre. Environmental science & technology. 2017; 51:13689–13697. [PubMed: 29161030]
14. Koelmans, AA, Besseling, E, Shim, WJ. Marine anthropogenic litter. Springer; 2015. 325–340.
15. Chávez JL, Wong JL, Duran RS. Core– shell nanoparticles: characterization and study of their use for the encapsulation of hydrophobic fluorescent dyes. Langmuir. 2008; 24:2064–2071. [PubMed: 18220429]
16. Dai S, Ravi P, Tam KC. Thermo-and photo-responsive polymeric systems. Soft Matter. 2009; 5:2513–2533.
17. Gruber, JV. Synthetic polymers in cosmeticsCosmetic Science and Technology Series. 1999. 217–274.
18. Günay KA, et al. Selective Peptide-Mediated Enhanced Deposition of Polymer Fragrance Delivery Systems on Human Hair. ACS applied materials & interfaces. 2017; 9:24238–24249. [PubMed: 28650615]
19. Murphy DS. Fabric softener technology: A review. Journal of Surfactants and Detergents. 2015; 18:199–204.
20. Hosseinkhani B, Callewaert C, Vanbeveren N, Boon N. Novel biocompatible nanocapsules for slow release of fragrances on the human skin. New biotechnology. 2015; 32:40–46. [PubMed: 25224920]

21. Rochman CM, et al. Scientific evidence supports a ban on microbeads. Environmental science & technology. 2015; 49:10759–10761. [PubMed: 26334581]
22. Dauvergne P. The power of environmental norms: marine plastic pollution and the politics of microbeads. Environmental Politics. 2018; 27:579–597.
23. Kole PJ, Löhr AJ, Van Belleghem FG, Ragas AM. Wear and tear of tyres: A stealthy source of microplastics in the environment. International journal of environmental research and public health. 2017; 14
24. Wagner S, et al. Tire wear particles in the aquatic environment-A review on generation, analysis, occurrence, fate and effects. Water research. 2018; 139:83–100. [PubMed: 29631188]
25. Soleimani M, et al. Smart polymer nanoparticles designed for environmentally compliant coatings. Journal of the American Chemical Society. 2011; 133:11299–11307. [PubMed: 21711057]
26. Vogelsang, C, , et al. Microplastics in road dust–characteristics, pathways and measures. Report No. 8257769665. NIVA - Norwegian Institute for Water Research; 2018.
27. Grass RN, et al. Tracking Trace Amounts of Submicrometer Silica Particles in Wastewaters and Activated Sludge Using Silica-Encapsulated DNA Barcodes. Environmental Science & Technology Letters. 2014; 1:484–489.
28. Rist S, Baun A, Hartmann NB. Ingestion of micro-and nanoplastics in Daphnia magna–Quantification of body burdens and assessment of feeding rates and reproduction. Environmental Pollution. 2017; 228:398–407. [PubMed: 28554029]
29. Vriens B, et al. Quantification of Element Fluxes in Wastewaters: A Nationwide Survey in Switzerland. Environmental science & technology. 2017; 51:10943–10953. [PubMed: 28671459]
30. Okubo, M. Macromolecular Symposia. Wiley Online Library; 307–325.
31. Beltzung A, et al. Incorporation and distribution of noble metal atoms in polyacrylonitrile colloidal particles using different polymerization strategies. Polymer. 2018; 145:41–53.
32. Ryu MS, et al. Prediction of Glass Transition Temperature and Design of Phase Diagrams of Butadiene Rubber and Styrene Butadiene Rubber via Molecular Dynamics Simulations. Physical Chemistry Chemical Physics. 2017
33. Becker, Y, Mendez, MP, Rodriguez, Y. Vision tecnologica. Citeseer;
34. Mao Y, Li S, Fang RL, Ploehn HJ. Magadiite/styrene-butadiene rubber composites for tire tread applications: Effects of varying layer spacing and alternate inorganic fillers. Journal of Applied Polymer Science. 2017; 134
35. Endo K. Synthesis and structure of poly (vinyl chloride). Progress in Polymer science. 2002; 27:2021–2054.
36. Moulay S. Chemical modification of poly(vinyl chloride)—Still on the run. Progress in Polymer Science. 2010; 35:303–331. DOI: 10.1016/j.progpolymsci.2009.12.001
37. Kulich, D, Gaggar, S, Lowry, V, Stepien, R. Acrylonitrile–butadiene–styrene polymers. Wiley Online Library; 2002.
38. Booth AM, Hansen BH, Frenzel M, Johnsen H, Altin D. Uptake and toxicity of methylmethacrylate-based nanoplastic particles in aquatic organisms. Environmental Toxicology and Chemistry. 2016; 35:1641–1649. [PubMed: 26011080]
39. Cole M, Lindeque P, Fileman E, Halsband C, Galloway T. The Impact of Polystyrene Microplastics on Feeding, Function and Fecundity in the Marine CopepodCalanus helgolandicus. Environmental science & technology. 2015; 49:1130–1137. [PubMed: 25563688]
40. Sures, B, Singer, C, Zimmermann, S. Palladium Emissions in the Environment. Springer; 2006. 489–499.
41. Besseling E, Quik JT, Sun M, Koelmans AA. Fate of nano-and microplastic in freshwater systems: A modeling study. Environmental Pollution. 2017; 220:540–548. [PubMed: 27743792]
42. Barton LE, Therezien M, Auffan M, Bottero J-Y, Wiesner MR. Theory and methodology for determining nanoparticle affinity for heteroaggregation in environmental matrices using batch measurements. Environmental Engineering Science. 2014; 31:421–427.
43. Geitner NK, O'Brien NJ, Turner AA, Cummins EJ, Wiesner MR. Measuring nanoparticle attachment efficiency in complex systems. Environmental Science & Technology. 2017; 51:13288–13294. [PubMed: 29043786]

44. Barton LE, Auffan M, Olivi L, Bottero J-Y, Wiesner MR. Heteroaggregation, transformation and fate of CeO 2 nanoparticles in wastewater treatment. Environmental Pollution. 2015; 203:122–129. [PubMed: 25875163]
45. Sun TY, et al. Envisioning Nano release dynamics in a changing world: using dynamic probabilistic modeling to assess future environmental emissions of engineered nanomaterials. Environmental science & technology. 2017; 51:2854–2863. [PubMed: 28157288]
46. Carr SA, Liu J, Tesoro AG. Transport and Fate of Microplastic Particles in Wastewater Treatment Plants. Water Research. 2016; 91:174–182. [PubMed: 26795302]
47. Murphy F, Ewins C, Carbonnier F, Quinn B. Wastewater treatment works (WwTW) as a source of microplastics in the aquatic environment. Environmental science & technology. 2016; 50:5800–5808. [PubMed: 27191224]
48. McCormick A, Hoellein TJ, Mason SA, Schluep J, Kelly JJ. Microplastic is an abundant and distinct microbial habitat in an urban river. Environmental science & technology. 2014; 48:11863–11871. [PubMed: 25230146]
49. Magnusson, K, Norén, F. Screening of microplastic particles in and down-stream a wastewater treatment plant. IVL Swedish Environmental Research Institute; 2014.
50. Browne MA, Galloway TS, Thompson RC. Spatial patterns of plastic debris along estuarine shorelines. Environmental Science & Technology. 2010; 44:3404–3409. [PubMed: 20377170]
51. Eriksen M, et al. Microplastic pollution in the surface waters of the Laurentian Great Lakes. Marine pollution bulletin. 2013; 77:177–182. [PubMed: 24449922]
52. Song YK, et al. Large accumulation of micro-sized synthetic polymer particles in the sea surface microlayer. Environmental science & technology. 2014; 48:9014–9021. [PubMed: 25059595]
53. Zhao S, Zhu L, Wang T, Li D. Suspended microplastics in the surface water of the Yangtze Estuary System, China: first observations on occurrence, distribution. Marine pollution bulletin. 2014; 86:562–568. [PubMed: 25023438]
54. Kaegi R, et al. Behavior of Metallic silver nanoparticles in a Pilot wastewater treatment plant. Environmental Science & Technology. 2011; 45:3902–3908. [PubMed: 21466186]
55. Westerhoff P, Song G, Hristovski K, Kiser MA. Occurrence and removal of titanium at full scale wastewater treatment plants: implications for TiO2 nanomaterials. Journal of Environmental Monitoring. 2011; 13:1195–1203. [PubMed: 21494702]
56. Koelmans AA, et al. Risks of plastic debris: unravelling fact, opinion, perception, and belief. Environmental science & technology. 2017; 51:11513–11519. [PubMed: 28971682]

Europe PMC Funders Author Manuscripts

Europe PMC Funders Author Manuscripts

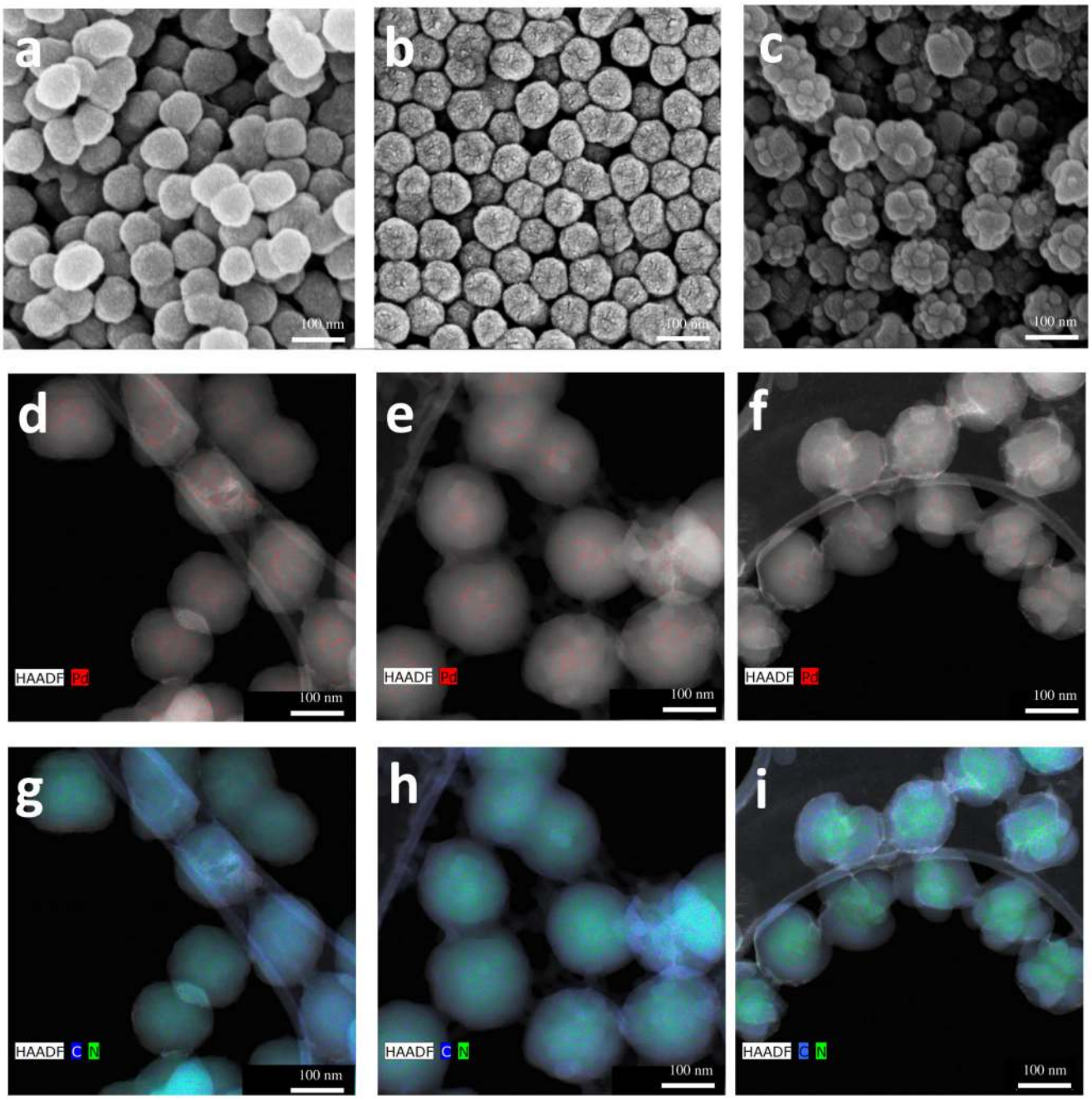

Figure 1.

SEM micrographs of typical nanoplastics; A) PAN Pd particle core, B) final core/shell particle with a smooth shell C) final core/shell particle with a raspberry-type shell. Elemental distribution maps of the various syntheses including: PAN core, smooth shell and raspberry shell exhibiting presence of Pd (HAADF and Pd Lα lines, enhanced), panels D, E, and F, respectively, and PAN core, smooth shell and raspberry shell exhibiting presence of N and C (HAADF and N, C K-lines, enhanced), panels G, H, and I, respectively. Pd (red) is predominantly detected only in the center of the particles (i.e. core). The core/shell structure

of the particles is notable with considerably more nitrogen (green) in the core of the particle from the acrylonitrile, with the outermost portion of the shell is entirely made of polystyrene (carbon only, blue). Note that the core sample pictured in Figure 1 panels A, D and G come from a separate synthesis and its size does not correspond to the core sizes belonging to the specific shell samples shown here. Additional images of HAADF and individual components (Pd, C, N, and O) and additional element combinations for all particles can be found in Figure S-4 with EDX in Figure S-5.

Europe PMC Funders Author Manuscripts

Europe PMC Funders Author Manuscripts

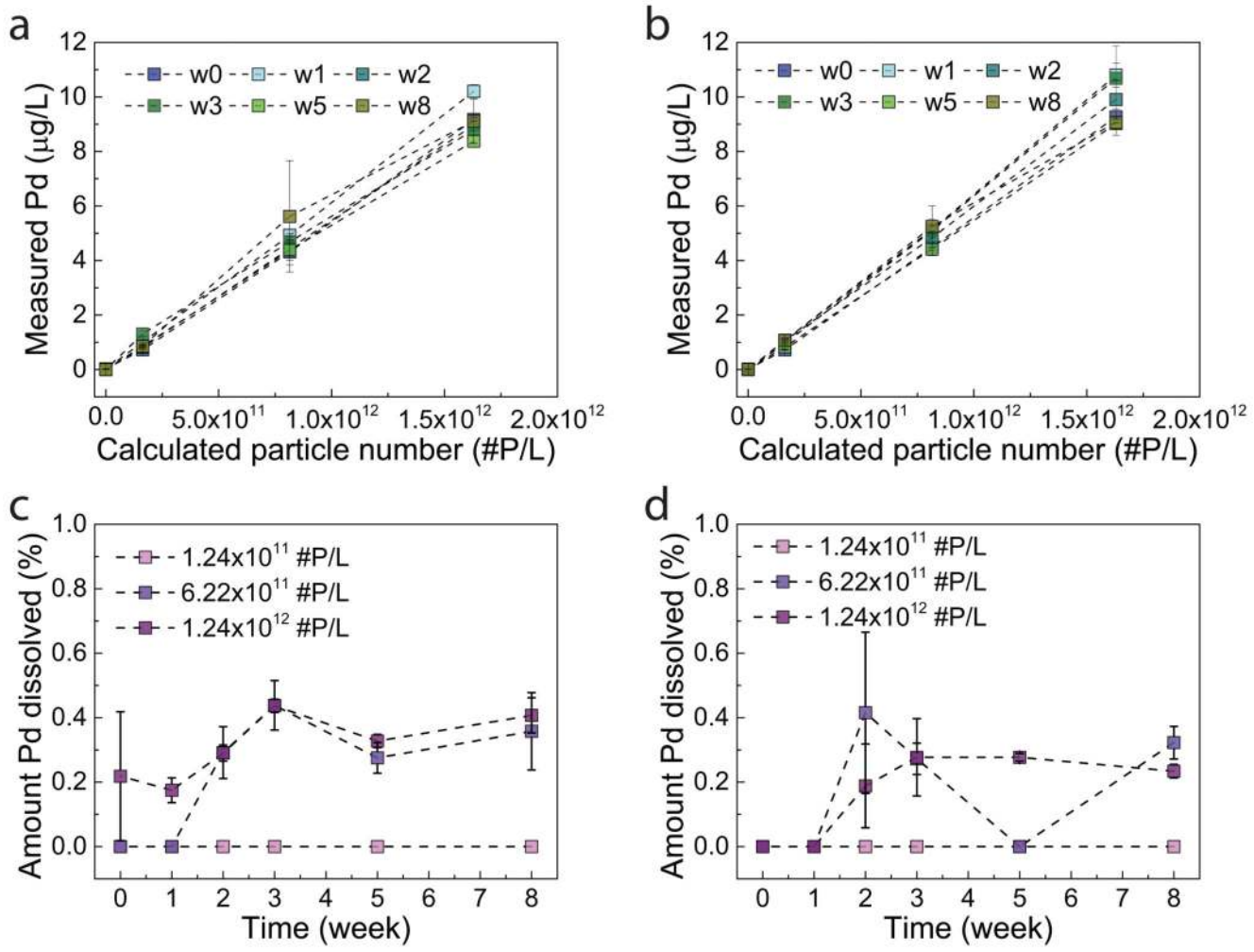

Figure 2.

By measuring the total Pd concentration of the same diluted suspension over time we can assess the general stability of the nanoplastics. Instability would include particles aggregating and settling, particles adhering to the vial walls, or leaching of the Pd tracer. Nanoplastic particle stability (top row) and Pd leaching potential (bottom row) over time, with particles diluted in DI water and shaking for multiple weeks (abbreviated “w”). Theoretical particle number concentrations calculated for the stock solution and scaled for various dilution factors (fixed over time), with subsequent weekly measurements of total Pd in solution of the raspberry shell (panel A) and smooth shell (panel B). The concentration of dissolved Pd measured in solution for the raspberry shell (panel C) and smooth shell (panel D) is presented in relation to the total Pd spiked into the suspension. Concentrations of Pd in solution at T=0 represent residual ionic Pd in the stock solution (i.e. Pd not incorporated into the particles during synthesis) and weekly measurements thereafter are indicative of additional leached Pd. All measurements below the detection limit were set to zero for graphing purposes. For core measurements, see Figure S-7.

Europe PMC Funders Author Manuscripts

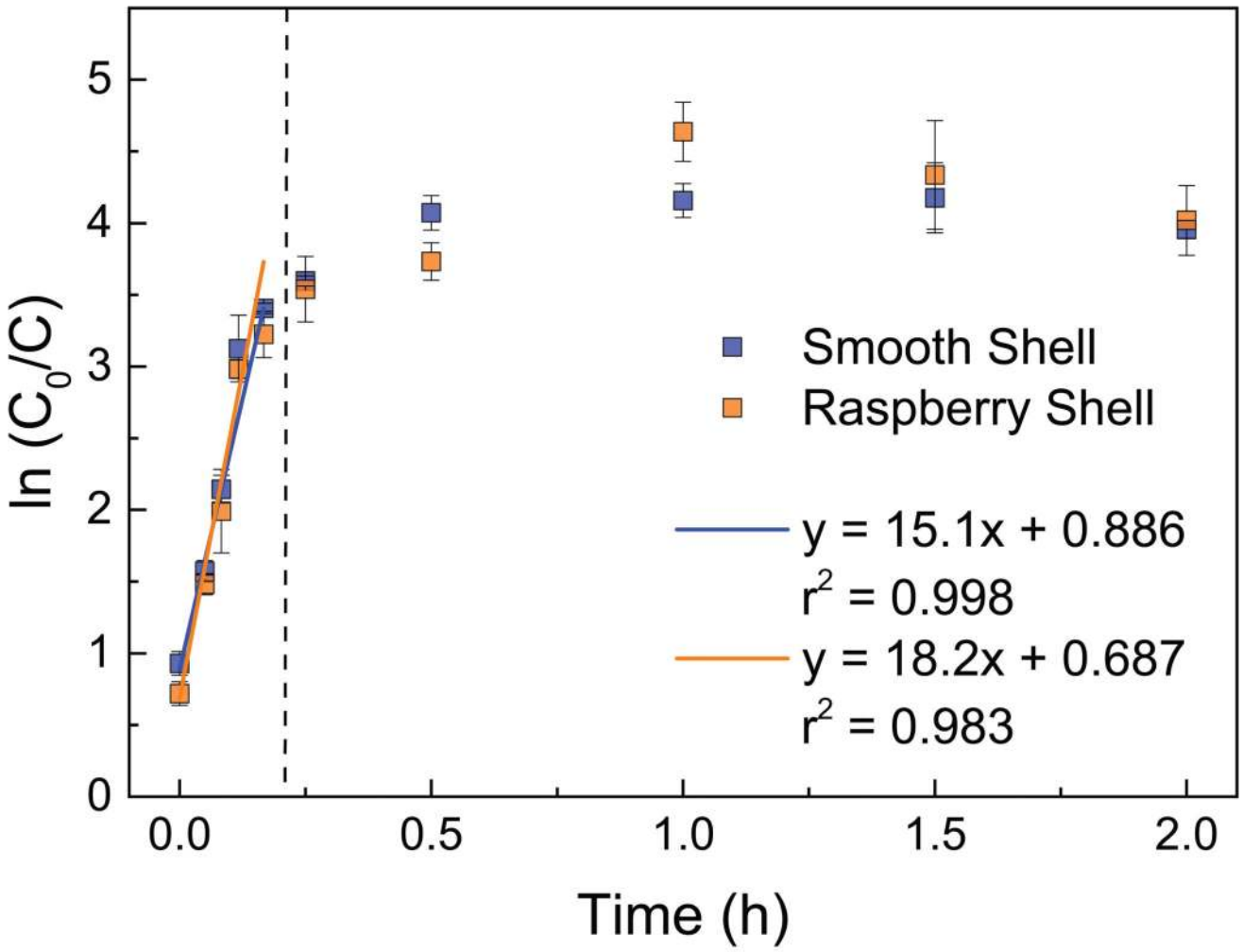

Figure 3.

Representative plot for smooth (blue) and raspberry (orange) shelled nanoplastics interacting with mixed liquor to illustrate removal with the sludge over time. The initial linear behavior that is used to assess heteroaggregation is shown for each material, indicated by time points less than 10 min with the dashed line. No statistical difference was noted between the different particles, indicating that the difference in surface morphology did not contribute greatly to the removal of nanoplastics in this instance over time spans that are relevant in our system of interest. Error bars indicate triplicate experiments.

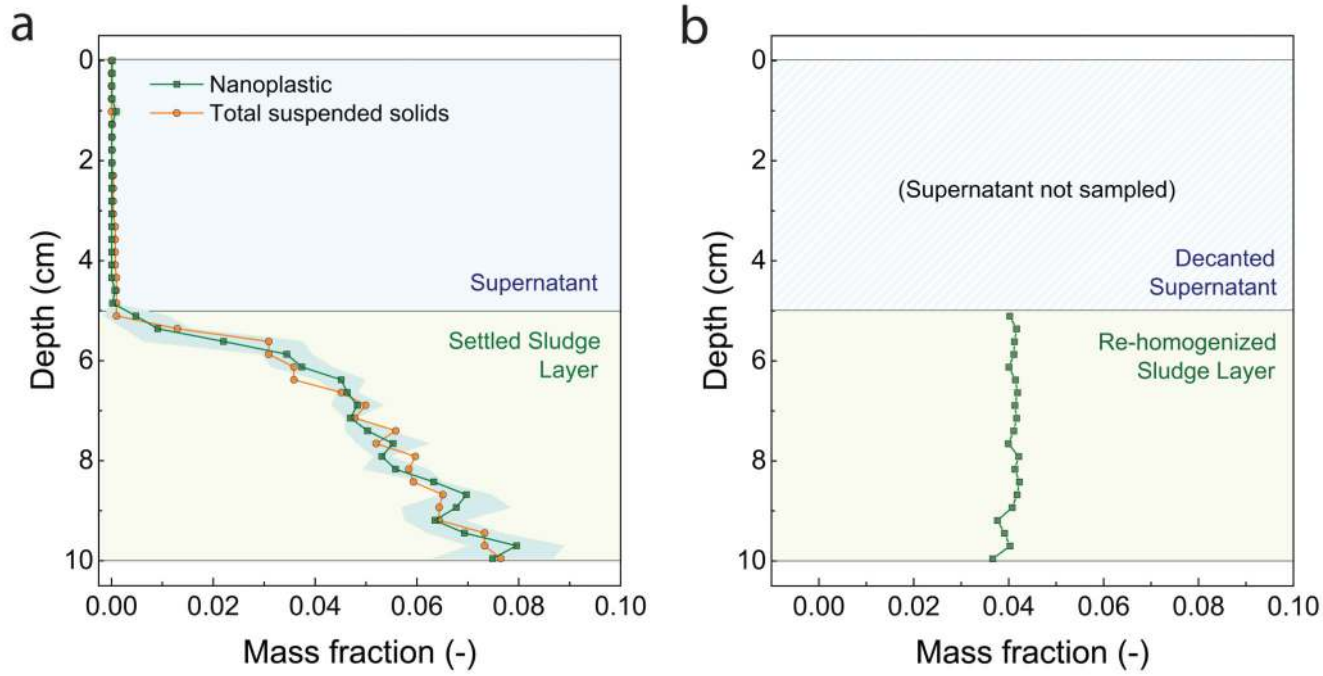

Figure 4.

(A) Depth profile of nanoplastic in batch reactor with settled activated sludge, representing the secondary clarifier treatment step of a municipal wastewater treatment plant. The x-axis shows the concentration of each component (nanoplastic or TSS) measured at a given sampling depth, normalized to the total concentration of the respective component in the system. The close correlation between the nanoplastic and TSS over depth indicates that nanoplastics have a high affinity for sludge, and there is a constant ratio between the two components. The blue background indicates supernatant with the green background indicated the sludge layer. Shaded zones around the measurements indicate error associated with triplicate experiments for three particle spike concentrations, which are averaged together here as the trend in nanoplastic attachment was independent of particle concentration tested. Nanoplastic recovery across all spiked additions was 93 +/- 3% (B) Re-homogenized sludge to eliminate TSS gradient in sludge layer, with subsequent sequential sampling to determine nanoplastic concentration with depth.

Europe PMC Funders Author Manuscripts